

Numerical Experiments in Plasma Focus Operated in Various Gases

Mohamad Akel, Sing Lee, and S. H. Saw

Abstract—We adapted the Lee Model code as a branch version RADPF5.15K to gases of special interest to us, namely, nitrogen and oxygen and applied numerical experiments specifically to our AECS PF-1 and AECS PF-2. We also generalized the numerical experiments to other machines and other gases to look at scaling laws and to explore recently uncovered insights and concepts. The required thermodynamic data of nitrogen, oxygen, neon, and argon gases (ion fraction, the effective ionic charge number, the effective specific heat ratio) were calculated, the X-ray emission properties of plasmas were studied, and suitable temperature range (window) for generating H- and He-like ions (therefore soft X-ray emissions) of different species of plasmas were found. The code is applied to characterize the AECS-PF-1 and AECS-PF-2, and for optimizing the nitrogen, oxygen, neon, and argon SXR yields. In numerical experiments we show that it is useful to reduce static inductance L_0 to a range of 15–25 nH; but not any smaller. These yields at diverse wavelength ranges are large enough to be of interest for applications. Scaling laws for argon and nitrogen SXR were found. Model parameters are determined by fitting computed with measured current waveforms in neon for INTI PF and in argon for the AECS PF-2. Radiative cooling effects are studied indicating that radiative collapse may be observed for heavy noble gases (Ar, Kr, Xe) for pinch currents even below 100 kA. The creation of the consequential extreme conditions of density and pulsed power is of interest for research and applications.

Index Terms—Lee Model, plasmas focus (PF), radiative collapse, scaling law, soft X-ray.

I. INTRODUCTION

SOFT X-ray sources of high intensity are required in diverse areas like X-ray spectroscopy [1], micro- lithography [2], X-ray microscopy [3], X-ray laser pumping [4], and X-ray crystallography [5]. Work is underway to develop such sources by employing geometries like Z-pinch [6], X-pinch [7], vacuum spark [8], and plasma focus (PF) [9]–[11]. The latter is the simplest in construction and yet provides the highest X-ray emission compared to other devices of equivalent energy [12], [13]. Efforts have been made for enhancing the X-ray yield by changing various experimental parameters such as bank energy [14], discharge current, electrode configuration (shape and material) [15], [16], insulator material and dimensions [15],

gas composition, and filling gas pressure [17] owing to possible applications including in materials [18]–[31].

Moreover, numerical experiments are gaining much interest. For example, the Institute of Plasma Focus Studies (IPFS) [32] conducted an International Internet Workshop on Plasma Focus Numerical Experiments [33], at which it was demonstrated that the Lee Model code [34] computes not only realistic focus pinch parameters, but also absolute values of SXR yield Y_{SXR} consistent with experimental measurements [13], [33]–[35]. Numerical experiments are also carried out systematically by Lee *et al.* [14], [36] to determine the neon Y_{SXR} for optimized conditions with storage energy E_0 from 1 kJ to 1 MJ. It is pointed out that the distinction of I_{pinch} from I_{peak} is of basic importance [37]–[39].

The Pease–Braginskii (P–B) current [40] is that current flowing in a hydrogen pinch which is just large enough for Bremsstrahlung to balance Joule heating. In gases emitting strongly in line radiation, the radiation-cooled threshold current is considerably lowered. Lee *et al.* showed that Lee Model code [34] may be used to compute this lowering [41], [42]. Ali *et al.* [43] reported that self absorption becomes significant when plasma is dense enough to be optically thick.

In this paper, we discuss the different states of X-ray radiative nitrogen, oxygen, neon and argon plasmas and their suitable working conditions in plasma focus. We discuss the laboratory measurements to determine model parameters. We discuss the comprehensive range of numerical experiments conducted to derive scaling laws on nitrogen and argon soft X-ray yield leading up the study of radiative collapse effect in the plasma focus.

II. CALCULATIONS OF PLASMA PARAMETERS USING CORONA MODEL

The X-ray radiation properties of plasmas are dependent on the plasma temperature, ionization states, and density. Plasma equilibrium model can be used to calculate the ion fraction α , the effective ionic charge number Z_{eff} , the effective specific heat ratio γ and X-ray emission of the plasma at different temperatures. The ion fraction is defined as the fraction of the plasma which is ionized to the z th ionized: $\alpha_z = N_z/N_i$ where: N_z is the z th ionized ion number density; N_i is the total ion number density. The effective ionic charge number Z_{eff} is the average charge of one ion [34], [44], [47]. Based on the corona model, we obtained for nitrogen, that the suitable temperature range for generating H-like 1s-2p, N_2 : 24.784 A° (500 eV), 1s-3p, N_2 : 21 A° (592.92 eV) and He-like 1s²-1s2p, N_2 : 89 29 A° (426 eV), 1s²-1s3p, N_2 : 24.96 A° (496 eV) ions in 89

Manuscript received April 29, 2012; revised July 15, 2012 and September 9, 2012; accepted September 18, 2012.

M. Akel is with the Department of Physics, Atomic Energy Commission, 6091 Damascus, Syria (makel@aec.org.sy, pscientific@aec.org.sy).

S. Lee is with the Institute for Plasma Focus Studies, Melbourne, VIC 3148, Australia and also with INTI International University, 71800 Nilai, Negeri Sembilan, Malaysia (e-mail:leesing@optusnet.com.au).

S. H. Saw is with the INTI International University, 71800 Nilai, Negeri Sembilan, Malaysia and also with the Institute for Plasma Focus Studies, Melbourne, VIC 3148, Australia (e-mail: sorheoh.saw@newinti.edu.my).

Digital Object Identifier 10.1109/TPS.2012.2220863

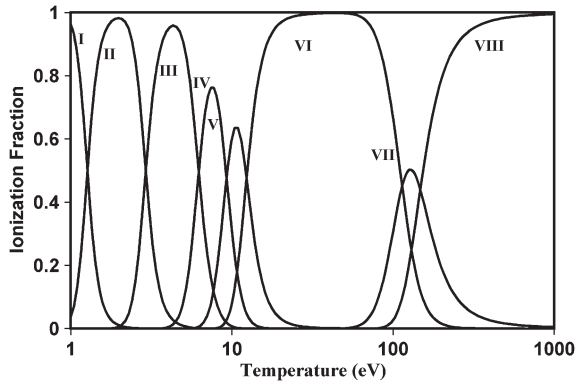


Fig. 1. Nitrogen ionization fractions as a function of temperature, where VIII indicates the ion N^{+7} [46].

90 nitrogen plasma (therefore, generating soft X-ray emission) is
91 74–173 eV ($0.86 \times 10^6 - 2 \times 10^6$ K)[46], [48]. It is also
92 noticed that the nitrogen atoms become fully ionized around
93 800 eV to 1000 eV.

94 The suitable temperature range for generating H-like 1s-2p,
95 O_2 : 18.97 A° (653.68 eV), 1s-3p, O_2 : 16 A° (774.634 eV)
96 and He-like $1s^2$ -1s2p, O_2 : 21.6 A° (573.947 eV), $1s^2$ -1s3p,
97 O_2 : 18.62 A° (665.615) ions in oxygen plasma (therefore, soft
98 X-ray emissions) has been calculated to be between 119 and
99 260 eV ($1.38 \times 10^6 - 3 \times 10^6$ K) with full ionization at around
100 2000 eV to 3000 eV [47].

101 For neon, a temperature window of 200eV to 500 eV ($2.3 \times$
102 $10^6 - 5 \times 10^6$ K) is suitable for generating H-like 1s-2p, Ne:
103 12.132 A° (1022 eV), 1s-3p, Ne: 10.240 A° (1211 eV) and
104 He-like $1s^2$ -1s2p, Ne: 13.447 A° (922 eV), $1s^2$ -1s3p, Ne:
105 11.544 A° (1074 eV) ions in neon plasma (therefore neon soft
106 X-ray emissions) [45], [49]–[51].

107 From the reported experimental results [44], [52], [53], the
108 X-ray emissions from argon plasma are mainly He-like alpha
109 line (He_α ($1s^2$ -1s2p, Ar: 3.9488 A° (3140 eV)), $1s^2$ -1s3p, Ar:
110 3.365 A° (3684 eV)) and H-like alpha line (Ly_α ($1s$ -2p, Ar:
111 3.731 A° (3323 eV)), ($1s$ -3p, Ar: 3.150 A° (3936 eV)) lines.
112 So, the most intense characteristic emissions of argon plasma
113 are Ly_α and He_α lines. The corresponding X-ray emitters
114 in the argon plasmas are mainly H- and He-like ions. For
115 argon, a focus pinch compression temperature of 1.4 keV to
116 5 keV ($16.3 \times 10^6 - 58.14 \times 10^6$ K) is suitable for generating
117 H- and He-like ions. An example of these calculations is shown
118 in Figs. 1 and 2.

119 Based on the above work we take the soft X-ray yield
120 (H- and He-like ions) from nitrogen, oxygen, neon and argon
121 to be equivalent to line radiation yield i.e., $Y_{srx} = Q_L$ at a
122 suitable different temperature ranges (T windows) for each
123 gas as follows: 74–173 eV for nitrogen [46], 119–260 eV for
124 oxygen [47], 200 to 500 eV for neon [49], [51], and for argon
125 is 1.4 keV to 5 keV [44], [52], [54].

126 III. NUMERICAL EXPERIMENTS USING LEE MODEL

127 A. Soft X-Ray Yield Versus Pressure

128 The dynamics of plasma focus discharges is complicated;
129 for this purpose, to investigate the plasma focus phenomena,

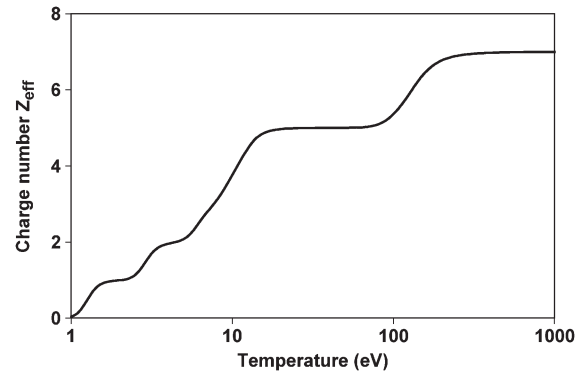


Fig. 2. Effective charge number Z_{eff} of N_2 calculated from Fig 1.

the Lee Model couples the electrical circuit with plasma focus 130
dynamics, thermodynamics and radiation, enabling realistic 131
simulation of all gross focus properties [34]–[36]. In the radial 132
phases, axial acceleration and ejection of mass are caused by 133
necking curvatures of the pinching current sheath result in time- 134
dependent strongly center-peaked density distributions. More- 135
over, laboratory measurements show that rapid plasma/current 136
disruptions result in localized regions of high densities and 137
temperatures particularly in the heavy gases like xenon. We 138
point out that these center-peaking density effects and localized 139
regions are not modeled in the code, which computes only an 140
average uniform density and an average uniform temperature 141
which are considerably lower than measured peak density and 142
temperature. However, because the four-model parameters are 143
obtained by fitting the computed total current waveform to 144
the measured total current waveform, the model incorporates 145
the energy and mass balances equivalent, at least in the gross 146
sense, to all the processes which are not even specifically 147
modeled. Hence, the computed gross features such as speeds 148
and trajectories and integrated soft X-ray yields have been ex- 149
tensively tested in numerical experiments for several machines 150
and are found to be comparable with measured values. Thus 151
the code provides a useful tool to conduct scoping studies, as 152
it is not purely a theoretical code, but offers means to conduct 153
phenomenological scaling studies for any plasma focus device 154
from low energy to high energy machines. 155

The Lee Model code has been successfully used to perform 156
numerical experiments to compute neon soft X-ray yield for 157
the NX2 as a function of pressure with reasonable degree of 158
agreement in (1) the Y_{srx} versus pressure curve trends, (2) the 159
absolute maximum yield, and (3) the optimum pressure value. 160
The only input required is a measured total current waveform. 161
This reasonably good agreement, against the background of 162
an extremely complicated situation to model, moreover the 163
difficulties in measuring Y_{srx} , gives confidence that the model 164
is sufficiently realistic in describing the plasma focus dynamics 165
and soft X-ray emission for NX2 operating in Neon. 166

In the code, line radiation Q_L is calculated as follows: 167

$$\frac{dQ_L}{dt} = -4.6 \times 10^{-31} N_i^2 Z_{eff}^4 (\pi a_{min}^2) Z_{max} / T$$

where for the temperatures of interest in our experiments we 168
take $Y_{srx} = Q_L$. 169

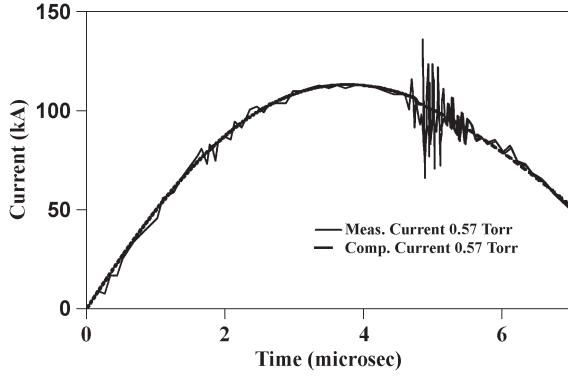


Fig. 3. Comparison of the computed current trace (smooth line) with the experimental one (solid line) of the AECS-PF-2 at 15 kV, 0.57 torr neon.

170 Hence, the SXR energy generated within the plasma pinch
 171 depends on the following properties: number density N_i , ef-
 172 fective charge number Z_{eff} , atomic number of gas Z_n , pinch
 173 radius a_{min} , pinch length Z_{max} , plasma temperature T and the
 174 pinch duration. This generated energy is then reduced by the
 175 plasma self-absorption which depends primarily on density and
 176 temperature; the reduced quantity of energy is then emitted as
 177 the soft X-ray yield.

178 As an example, in the modified Lee Model code version,
 179 we take the nitrogen soft X-ray yield to be equivalent to
 180 line radiation yield i.e., $Y_{sxr} = Q_L$ at the following tem-
 181 perature range 74–173 keV. In any shot, for the duration
 182 of the focus pinch, whenever the focus pinch temperature
 183 is within this range, the line radiation is counted as nitro-
 184 gen soft X-rays. Whenever the pinch temperature is outside
 185 this range, the line radiation is not included as nitrogen soft
 186 X-rays.

187 For the plasma column, using Spitzer form for resistivity, and
 188 the Bennett distribution we obtain a relationship between T and
 189 I as follows:

$$T = b \frac{I^2}{(n_i r_p^2) (1 + Z_{eff})}$$

$$\text{where } b = \frac{\mu}{8\pi^2 k}.$$

190 Numerical experiments have been investigated systemati-
 191 cally using Lee Model to characterize various low energy
 192 plasma focus devices operated with different gases (nitrogen,
 193 oxygen, neon, argon) and plasma focus parameters.

194 For each studied plasma focus device, fitted values of the
 195 model parameters were found using the following procedures:
 196 The computed total discharge current waveform is fitted to the
 197 measured by varying model parameters f_m , f_c , f_{mr} and f_{cr} one
 198 by one until the computed waveform agrees with the measured
 199 waveform [55].

200 For example, experiments have been investigated on the
 201 AECS-PF-2 with Ne at wide range of pressures to get exper-
 202 imental current traces with good focus effect [63] from 0.25 to
 203 1.25 torr. To start the numerical experiments we select a dis-
 204 charge current trace of the AECS-PF-2 taken with a Rogowski
 205 coil at 0.57 torr (Fig. 3).

We configure the Lee Model code (version RADPF5.15K) to 206
 operate as the AECS-PF-2 plasma focus. To obtain a reasonably 207
 good fit the following parameters are used: 208

Bank parameters: static inductance $L_0 = 280$ nH, capacitance 209
 $C_0 = 25$ μ F, stray resistance $r_0 = 25$ m Ω , 210

Tube parameters: cathode radius $b = 3.2$ cm, anode radius $a = 211$
 0.95 cm, anode length $z_0 = 16$ cm, 212

Operating parameters: voltage $V_0 = 15$ kV, pressure $p_0 = 213$
 0.57 torr, Ne gas, together with the following fitted model 214
 parameters: 215

$$f_m = 0.1, f_c = 0.7, f_{mr} = 0.2 \text{ and } f_{cr} = 0.7.$$

With these parameters, the computed total current trace 216
 agrees reasonably well with the experimental trace (Fig. 3). 217

These fitted values of the model parameters are then used for 218
 the computation of all the discharges at pressures from 0.1 to 219
 2.1 torr [63]. The results (Table I) show that the Y_{sxr} attains an 220
 optimum value of 0.42 J at 1.12 torr (efficiency 0.015%, end 221
 axial speed $V_a = 4.2$ cm/ μ s, speed factor (SF) is 113.4 kA/cm 222
 per [torr of Ne] $^{1/2}$) [11]. 223

It is evident from Table I that the peak value of total dis- 224
 charge current I_{peak} decreases with decreasing pressure. This 225
 is due to increasing dynamic resistance (rate of change of tube 226
 inductance, dL/dt gives rise to a dynamic resistance equal to 227
 0.5 dL/dt [36]) due to increasing current sheath speed as pres- 228
 sure is decreased. On the contrary, the current I_{pinch} that flows 229
 through the pinched plasma column increases with decreasing 230
 pressure until it reaches the maximum. This is due to the 231
 shifting of the pinch time towards the time of peak current as 232
 the current sheet moves faster and faster. As the pressure is 233
 decreased, the increase in I_{pinch} may be expected to favor Y_{sxr} ; 234
 however there is a competing effect that decreasing pressure 235
 reduces the number density. The interaction of these competing 236
 effects will decide on the actual yield versus pressure [49], 237
 [51]. The Lee Model code was also applied to characterize the 238
 UNU/ICTP PFF Plasma Focus, finding a maximum argon soft 239
 X-ray yield (Y_{sxr}) of 0.039 J [63]. 240

B. Soft X-Ray Yield Versus Electrode Geometry 241

We next optimize Y_{sxr} from various plasma focus devices 242
 with different gases. More numerical experiments were carried 243
 out; varying p_0 , z_0 and “a” keeping $c = b/a$ constant. The 244
 pressure p_0 was slightly varied. The following procedure was 245
 used [46], [47], [49], [51], [52], [55]. At each p_0 , the anode 246
 length z_0 was fixed at a certain value; then the anode radius “a” 247
 was varied, till the maximum Y_{sxr} was obtained for this z_0 . This 248
 was repeated for other values of z_0 , until we found the optimum 249
 combination of z_0 and “a” at the fixed p_0 . Then we changed p_0 250
 and repeated the above procedure; until finally we obtained the 251
 optimum combination of p_0 , z_0 and “a”. 252

The optimized results for each value of p_0 showed that 253
 as p_0 is increased, “a” has to be decreased to maintain the 254
 required speeds so that the argon pinch remains within the 255
 required temperature window. The Y_{sxr} attains an optimum 256
 value of 0.0035 J at $p_0 = 1.8$ torr as shown in Fig. 4 which 257
 also shows corresponding optimum end axial speed as with 258

TABLE I

VARIATION AECS-PF-2 PARAMETERS WITH PRESSURE AT: $L_0 = 280$ nH, $C_0 = 25$ μ F, $r_0 = 25$ m Ω , $V_0 = 15$ kV, RATIO OF STRAY RESISTANCE/BANK SURGE IMPEDANCE $RESF = 0.24$, $c = b/a = 3.37$, $f_m = 0.1$, $f_c = 0.7$, $f_{mr} = 0.2$, $f_{cr} = 0.7$, NEON GAS [63]

p_0 (Torr)	I_{peak} (kA)	I_{pinch} (kA)	V_a (cm/ μ s)	V_s (cm/ μ s)	V_p (cm/ μ s)	SF	Pinch duration(ns)	Y_{srx} (J)	Efficiency (%)
2.1	The code unable to run								
1.30	114.4	61.9	3.88	19.9	14.2	105.6	9.2	0.000	0
1.20	114.2	64.4	4.06	21.5	14.7	109.7	8.6	0.000	0
1.15	114.1	65.6	4.16	22.5	15.0	112.0	8.2	0.000	0
1.12	114.0	66.3	4.22	23.2	15.2	113.4	8.0	0.418	0.015
1.10	114.0	66.8	4.27	23.7	15.3	114.4	7.7	0.355	0.013
1.00	113.8	69.0	4.49	24.9	15.8	119.8	7.9	0.247	0.009
0.80	113.2	72.8	5.03	25.8	16.9	133.2	8.2	0.114	0.004
0.70	112.8	74.4	5.36	26.8	17.8	141.9	8.2	0.075	0.0026
0.57	112.2	75.9	5.87	28.7	19.6	156.4	7.9	0.039	0.0014
0.50	111.7	76.4	6.21	30.1	20.9	166.3	7.6	0.026	0.0009
0.40	111.0	76.5	6.80	32.8	23.4	184.7	7.0	0.013	0.0005
0.30	109.5	75.7	7.59	35.9	26.2	210.3	6.5	0.005	0.0002
0.20	105.6	73.2	8.78	41.7	30.0	248.5	5.7	0.001	0.000036
0.10	96.2	66.8	11.04	52.7	36.8	320.1	4.6	0.000	0

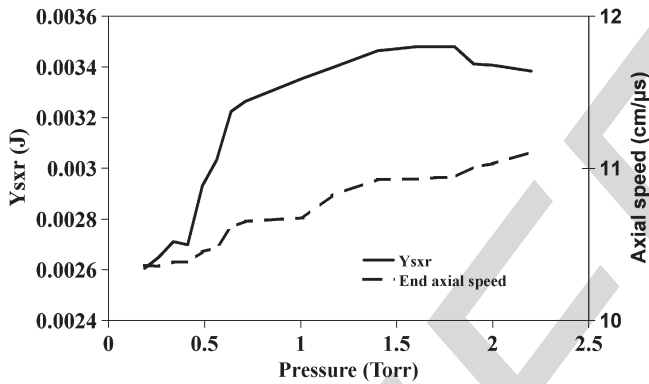


Fig. 4. Y_{srx} and end axial speed of AECS-PF-2 in Ar (Y_{srx} versus p_0 , optimized z_0 and “a” for each point) [52].

259 the plasma focus operated at the optimum combination of z_0
 260 and “a” corresponding to each p_0 . We thus found for the
 261 AECS-PF-2 the optimum combination of p_0 , z_0 and “a” for
 262 argon Y_{srx} as 1.8 torr, 24.3 cm and 0.26 cm, respectively, with
 263 the outer radius $b = 0.9$ cm. This combination gives $Y_{srx} =$
 264 0.0035 J with $I_{peak} = 102$ kA, $I_{pinch} = 71$ kA, and end axial
 265 speed is of 11 cm/ μ s [52].

266 Practically, it is technically difficult to change “b”; unless
 267 the whole electrode and input flange system is completely
 268 redesigned. So, for practical optimization, we wish to [49], [52],
 269 [63] keep $b = 3.2$ cm and compute the optimum combinations
 270 of (p_0 , “a”), (p_0 , z_0) and (p_0 , z_0 , “a”) for the maximum Y_{srx} .
 271 This gives us a practical optimum configuration of $b = 3.2$ cm,
 272 $a = 1.567$ cm, $z_0 = 9$ cm, giving a practical optimum yield of
 273 0.924 J at 0.58 torr for Ne [63].

274 C. Soft X-Ray Yield Versus Inductance

275 We investigated the effect of reducing L_0 down to 3 nH
 276 [38], [39], [48], [49], [52], [63], [64] for different plasma
 277 focus devices operated with various gases. For example, it was

TABLE II

FOR EACH L_0 , THE OPTIMIZED COMBINATION OF z_0 AND “A” WERE FOUND AND ARE LISTED HERE. $L_0 = 280$ nH, $C_0 = 25$ μ F, $r_0 = 25$ m Ω ; $c = b/a = 3.37$; MODEL PARAMETERS: $f_m = 0.1$, $f_c = 0.7$, $f_{mr} = 0.2$, $f_{cr} = 0.7$; 2.8 torr Ne, $V_0 = 15$ kV

L_0 (nH)	z_0 (cm)	a (cm)	b (cm)	I_{peak} (kA)	I_{pinch} (kA)	a_{min} (cm)	Z_{max} (cm)	V_a (cm/ μ s)	Y_{srx} (J)
280	8.00	0.727	2.45	115	79	0.05	1.0	3.45	0.94
200	7.00	0.842	2.84	135	92	0.06	1.2	3.52	1.66
100	4.50	1.125	3.79	186	125	0.08	1.6	3.57	5.16
50	4.00	1.400	4.73	256	158	0.10	2.0	4.02	11.62
25	2.80	1.640	5.52	340	190	0.14	2.4	4.50	18.72
20	2.50	1.693	5.70	369	198	0.16	2.5	4.72	20.35
15	2.40	1.732	5.83	410	205	0.17	2.6	5.15	21.77
10	2.00	1.760	5.93	464	212	0.20	2.7	5.71	21.40
5	1.97	1.749	5.89	556	214	0.25	2.7	7.12	16.14
3	1.96	1.705	5.74	608	211	0.26	2.6	8.16	13.19

found that reducing L_0 increases the total current from $I_{peak} = 278$
 115 kA at $L_0 = 280$ nH to $I_{peak} = 410$ kA at $L_0 = 15$ nH for
 AECS-PF-2 with neon gas [63] (see Table II). 280

As L_0 was reduced, I_{peak} increased; “a” is necessarily in-
 creased leading to longer pinch length (z_{max}), hence a bigger
 pinch inductance L_p . At the same time because of the reducing
 current drive time, z_0 needed to be reduced. The geometry
 moved from a long thin Mather-type to a shorter fatter one.
 Thus while L_0 and axial section inductance L_a reduced, the
 pinch inductance L_p increased due to increased pinch length
 [38], [48], [63]. 288

While I_{peak} increases with each reduction in L_0 with no
 sign of any limitation, I_{pinch} reaches a maximum of 214 kA at
 $L_0 = 5$ nH, then it decreases with each reduction in L_0 . From
 Table II it can be seen, that as L_0 decreased, Y_{srx} increases until
 it reaches a maximum value of 22 J at $L_0 = 15$ nH; beyond
 which Y_{srx} does not increase with reducing L_0 . This confirms
 the pinch current and Y_{srx} limitation effect in Ne plasma focus. 295

Based on the results of these numerical experiments on
 various devices with different gases, to improve Y_{srx} , L_0 should 297

TABLE III

OPTIMIZED CONFIGURATION FOUND FOR EACH E_0 ; $L_0 = 10$ nH,
 $V_0 = 15$ kV, 1 torr ARGON; f_m, f_c, f_{mr}, f_{cr} ARE FIXED AT 0.05, 0.7, 0.15
 AND 0.7 RESPECTIVELY, v_a IS THE PEAK AXIAL SPEED

E_0 (kJ)	C_0 (μ F)	a (cm)	z_0 (cm)	I_{peak} (kA)	I_{pinch} (kA)	v_a (cm/ μ s)	Y_{sxx} (J)	Efficiency (%)
1.1	10	0.70	4	251.4	148.8	13.60	0.05	0.0045
2.8	25	0.90	6	329.5	193.1	13.98	0.13	0.0046
4.5	40	1.01	8	370.7	217.1	14.08	0.22	0.0048
5.6	50	1.07	9	390.4	229.0	14.08	0.26	0.0046
11.3	100	1.24	15	448.8	264.3	14.03	0.52	0.0046
22.5	200	1.41	23	503.5	300.1	13.79	1.01	0.0045
45.0	400	1.58	37	551.9	333.6	13.46	1.85	0.0041
67.5	600	1.68	43	578.3	354.5	13.30	2.52	0.0037
90.0	800	1.74	57	594.5	366.1	13.11	3.15	0.0035
112.5	1000	1.80	61	607.3	377.2	13.03	3.72	0.0033
450.0	4000	2.07	133	669.8	432.4	12.48	7.67	0.0020
900.0	8000	2.18	177	692.4	454.9	12.30	9.66	0.0010
1012.5	9000	2.20	209	695.7	457.8	12.24	10.03	0.0001

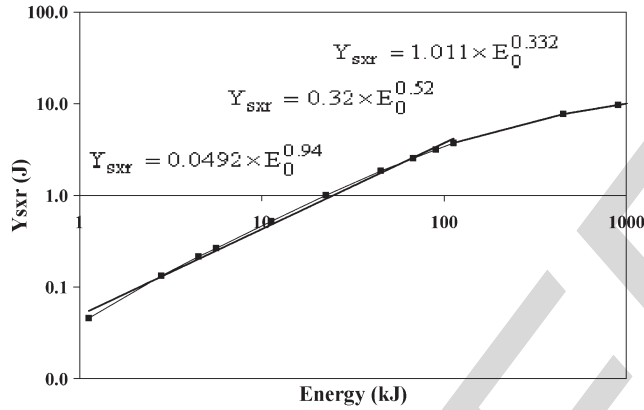


Fig. 5. Y_{sxx} versus E_0 . The parameters kept constants are: RESF = 0.337, $c = 3.37$, $L_0 = 10$ nH, $p_0 = 1$ torr Argon and $V_0 = 15$ kV and model parameters f_m, f_c, f_{mr}, f_{cr} at 0.05, 0.7, 0.15 and 0.7, respectively [53].

298 be reduced to a value around 15–25 nH, which is an achievable
 299 range incorporating low inductance technology, below which
 300 I_{pinch} and Y_{sxx} would not be improved.

301 D. Scaling Laws for Soft X-Ray Yield of Argon 302 and Nitrogen Plasma Focus

303 Following above stated procedures numerical experiments
 304 were investigated on AECS-PF-2 like argon plasma focus at
 305 different operational gas pressures (0.41, 0.75, 1, 1.5, 2.5, and
 306 3 torr) for two different static inductance values L_0 (270 and
 307 10 nH) and then after systematically carrying out more than
 308 3000 numerical runs, the optimized conditions are obtained.
 309 Table III shows optimized configuration found for each E_0 for
 310 10 nH at gas pressure of 1 torr. From this data, we also plot Y_{sxx}
 311 against E_0 as shown in Fig. 5 to obtain scaling law: $Y_{sxx} =$
 312 $0.05E_0^{0.94}$ in the 1 to 100 kJ regions. The scaling deteriorates
 313 as E_0 is increased to $Y_{sxx} = 0.32E_0^{0.52}$, and then to $Y_{sxx} =$
 314 $1.01E_0^{0.33}$ at high energies towards 1 MJ. The requirement of a
 315 temperature window for the pinch fixes the axial speed within a
 316 narrow range of values. This fixes the axial dynamic resistance
 317 to a value around 7 m Ω for a plasma focus of any size. However,
 318 as E_0 is increased by increasing C_0 , the bank surge impedance

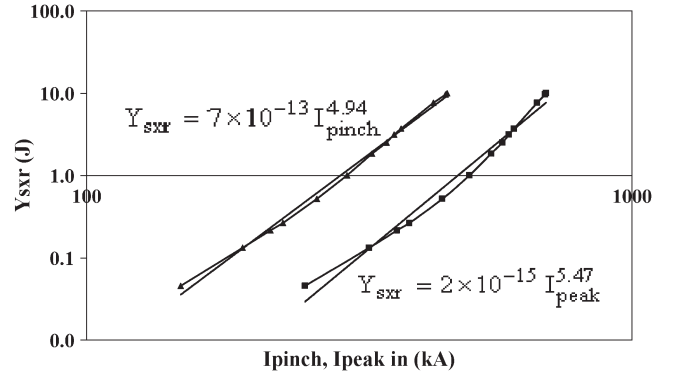


Fig. 6. Y_{sxx} versus I_{pinch}, I_{peak} . The parameters kept constants are: RESF = 0.337, $c = 3.37$, $L_0 = 10$ nH, $p_0 = 1$ torr Ar and $V_0 = 15$ kV and model parameters f_m, f_c, f_{mr}, f_{cr} at 0.05, 0.7, 0.15 and 0.7 [53]

$Z_0 = (L_0/C_0)^{0.5}$ ranges from 30 m Ω (for 1 kJ) to 1 m Ω (for 319
 1 MJ). Thus at 1 kJ the plasma focus current is dominated by 320
 the bank impedance while at 1 MJ the bank impedance hardly 321
 affects the discharge current. At 1 kJ quadrupling C_0 322
 would double I_{peak} ; but at 1 MJ quadrupling C_0 would increase 323
 I_{peak} by only some 7%. This is what causes the deterioration 324
 of current scaling with respect to E_0 . 325

This is consistent with the deterioration of scaling with 326
 increasing E_0 in the case of neutron yield attributed to reduction 327
 of current rise due to the increasingly dominant effect of the 328
 dynamic resistance [65], [66]. Our results indicate that such 329
 yield deterioration with increasing E_0 is a general effect appli- 330
 cable to not just neutrons but also to SXR yields. We then plot 331
 Y_{sxx} against I_{peak} and I_{pinch} and obtain Fig. 6 which shows 332
 $Y_{sxx} = 7 \times 10^{-13} I_{pinch}^{4.94}$ and $Y_{sxx} = 2 \times 10^{-15} I_{peak}^{5.47}$ [53]. 333

Scaling laws for N₂ [67] and Ne soft X-ray yields [14], [36], 334
 in terms of storage energies E_0 , were found to be best averaged 335
 as $Y_{sxxN} = 1.93E_0^{1.21}$ and $Y_{sxxNe} = 11E_0^{1.2}$ (yield in J, E_0 in 336
 kJ), respectively at energies in the 2 to 400 kJ regions. By 337
 comparing our recent results for N₂ plasma focus with Ar and 338
 Ne soft X-ray yields over this studied storage energy ranges, it 339
 is seen that the Ne soft X-ray yield of plasma focus is the most 340
 intense one (Fig. 7). The plasma focus is a powerful source of 341
 X-rays with wavelengths which may be suitably selected for 342
 microlithography, micromachining and microscopy simply by 343
 selecting the working gas (Ne or Ar or N₂ correspondingly) and 344
 choosing corresponding design and operating parameters of the 345
 device. 346

E. Model Parameters Versus Gas Pressure in Two Different Plasma Focus Devices Operated in Argon and Neon 347

Using the Lee Model, the computed and measured current 349
 are fitted varying the pressure, with the purpose to find the 350
 proper model parameters versus pressure for AECS-PF-2 and 351
 INTI PF devices operated with Ar and Ne, respectively. The 352
 results show a value of $f_m = 0.05 \pm 0.01$ over the whole range 353
 of pressure 0.2–1.2 torr in Ar; and $f_m = 0.04 \pm 0.01$ over 354
 0.7–4.1 torr in Ne. The value of $f_c = 0.7$ was fitted for all 355
 cases. Combining these results with those published for several 356
 other small machines, where measured current waveforms are 357

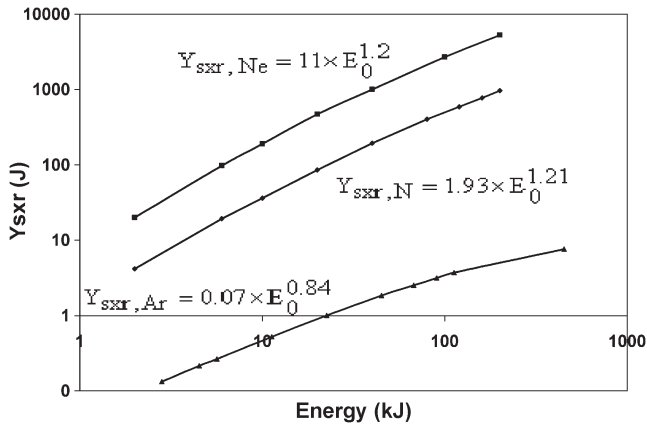


Fig. 7. Soft X-ray yields versus storage energy for Ne, N₂ and Ar plasma focus [67].

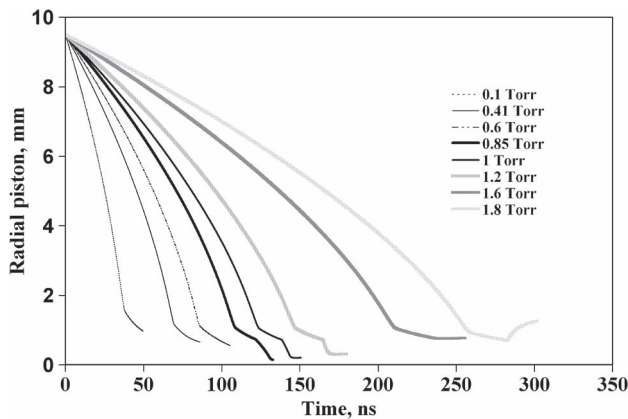


Fig. 8. Variations of radial piston trajectories on AECS-PF-2 for different Ar pressure [66] showing a regime of radiative collapse.

358 not available, a good compromise would be to take a guideline
359 value of $f_m = 0.05$ and $f_c = 0.7$ for both Ar and Ne [55].

360 F. Radiative Collapse in Plasma Focus Operated With 361 Heavy Noble gases

362 Numerical experiments have been investigated on plasma
363 focus device to study radiative collapse phenomena.

364 Fig. 8 shows variations of radial trajectories versus pressures
365 on AECS-PF-2 device. At 0.85 torr and a pinch temperature
366 of 190 eV with a pinch current of just under 66 kA, radiative
367 collapse is obvious with the radius collapsing in a few ns to the
368 cutoff radius of 0.1 mm set in the model. At lower pressures
369 such as 0.41 torr and higher pressures such as 1.6 torr clearly
370 the pinch compression is far less. The range of 0.85 to 1.2 torr
371 is when the radiation is maximum due to both factors of high
372 pinch density as well as sufficiently large pinch current. Above
373 1.2 torr the pinch is coming too late in the discharge cycle and
374 although the density is higher the current is already too low to
375 cause sufficient radiation to lead to radiative collapse.

376 Finally, based on obtained results by five phase Lee Model,
377 we can say that gas type and pressure of the plasma focus
378 play an important role in radiative collapse creation. This
379 phenomenon produces an extreme increase in tube voltage and
380 generates huge line radiations in the plasma focus [68].

IV. CONCLUSION

381

The Lee Model code has been adapted to N₂ and O₂. We
382 applied the numerical experiments specifically to our AECS-
383 PF-1 and AECS-PF-2. Numerical experiments have been gen-
384 eralized to other machines and other gases to look at scaling
385 and scaling laws and to explore recently uncovered insights
386 and concepts. The required thermodynamic data of N₂, O₂,
387 Ne and Ar gases at different temperatures were calculated, the
388 X-ray emission properties of plasmas were studied and suitable
389 temperature range (window) for generating H- and He-like ions
390 in the various gases. 391

The Lee Model code version RADPF5.15K is used to char-
392 acterize the AECS-PF-1 and AECS-PF-2, and for optimizing
393 the N₂, O₂, Ne, and Ar SXR yields. 394

Numerical experiments show the big influence of L₀ for
395 improving the soft X-ray yield; that it is useful to reduce L₀
396 to a range of 15–25 nH; but not any smaller since further
397 reduction produces no yield benefit and would be a futile
398 expensive exercise. For our machines, reduction of L₀ would
399 give the optimum soft X-ray yields from N₂, O₂, Ne and Ar
400 of 6 J, 10 J, 22 J, and 0.1 J, respectively. These yields at
401 diverse wavelength ranges are large enough to be of interest
402 for applications ranging from microelectronics lithography to
403 micro-machining and microscopy of biological specimens. 404

Scaling laws for SXR of Ar and N₂ plasma focus, in terms of
405 energy, peak and focus pinch current were found. 406

Numerical experiments were carried out on different plasma
407 focus devices with different filling gases to show that radiation
408 cooling and radiative collapse may be observed for heavy noble
409 gases (Ar, Kr, Xe) for pinch currents even below 100 kA. 410
The results show that the line radiation emission and tube
411 voltages have huge values near the radiative collapse regime. 412
The creation of the consequential extreme conditions of density
413 and pulsed power is of interest for research and applications. 414
Current waveforms and SXR measurements in krypton [41] are
415 being evaluated to study such radiative conditions. 416

ACKNOWLEDGMENT

417

The authors would like to thank Director General of AECS,
418 for encouragement and permanent support. 419

REFERENCES

420

- [1] J. S. Pearlman and J. C. Roirdan, "X-ray lithography using a pulsed plasma
421 source," *J. Vac. Sci. Technol.*, vol. 19, no. 4, pp. 1190–1193, Nov. 1981. 422
- [2] J. S. Pearlman, J. C. Riordan, and J. L. Costa, "Flash X-ray microscopy with
423 a gas jet plasma source," *J. Microsc.*, vol. 135, no. 3, pp. 347–351, Sep. 1984. 424
- [3] B. Niemann, D. Rudolph, G. Schmahl, M. Diehl, J. Thieme, 425
W. Meyer-Illse, W. Neff, R. Holz, R. Lebert, F. Richter, and G. Herziger,
426 "An X-ray microscope with a plasma source," *Optik*, vol. 84, no. 1, 427
pp. 35–36, 1990. 428
- [4] J. L. Porter, R. B. Spielman, M. K. Matzen, E. J. McGuire, L. E. Ruggles,
429 M. F. Vargas, J. P. Apruzese, R. W. Clark, and J. Davis, "Demonstration
430 of population inversion by resonant photopumping in a neon gas
431 cell irradiated by a sodium Z pinch," *Phys. Rev. Lett.*, vol. 68, no. 6, 432
pp. 796–799, Feb. 1992. 433
- [5] J. J. Rocca, V. Shlyaptsev, F. G. Tomasel, O. D. Cortázar, D. Hartshorn,
434 and J. L. A. Chilla, "Demonstration of a discharge pumped table-top soft-
435 X-ray laser," *Phys. Rev. Lett.*, vol. 73, no. 16, pp. 2192–2195, Oct. 1994. 436
- [6] V. L. Kantsyrev, K. I. Kopytok, and A. S. Shlyaptseva, "Results of
437 the study of the new type of compact gas-puff plasma source of SXR
438 (Soft X-ray)," in *Proc. 3rd Int. Conf. Dense Z-Pinches*, M. Haines and
439 A. Knight, Eds., 1993, vol. 299, pp. 226–230. 440

- [7] D. A. Hammer, D. H. Kalantar, K. C. Mittal, and N. Qi, "X-pinch soft X-ray source for microlithography," *Appl. Phys. Lett.*, vol. 57, no. 20, pp. 2083–2085, Nov. 1990.
- [8] C. S. Wong and S. Lee, "Vacuum spark as a reproducible X-ray source," *Rev. Sci. Instrum.*, vol. 55, no. 7, pp. 1125–1128, Jul. 1984.
- [9] J. W. Mather, "Formation of a high-density deuterium plasma focus," *Phys. Fluids*, vol. 8, no. 2, pp. 366–377, Feb. 1965.
- [10] S. Lee, T. Y. Tou, S. P. Moo, M. A. Eissa, A. V. Gholap, K. H. Kwek, S. Mulyodrono, A. J. Smith, Suryadi, W. Usada, and M. Zakauallah, "A simple facility for the teaching of plasma dynamics and plasma nuclear fusion," *Amer. J. Phys.*, vol. 56, no. 1, pp. 62–68, Jan. 1988.
- [11] S. Lee and A. Serban, "Dimensions and lifetime of the plasma focus pinch," *IEEE Trans. Plasma Sci.*, vol. 24, no. 3, pp. 1101–1105, Jun. 1996.
- [12] M. M. Zakauallah, K. Alamgir, M. Shafiq, S. M. Hassan, M. Sharif, and A. Waheed, "Enhanced copper K-alpha radiation from a low-energy plasma focus," *Appl. Phys. Lett.*, vol. 78, no. 7, pp. 877–879, Feb. 2001.
- [13] S. Lee, P. Lee, G. Zhang, X. Feng, V. A. Gribkov, M. Liu, A. Serban, and T. K. S. Wong, "High rep rate high performance plasma focus as a powerful radiation source," *IEEE Trans. Plasma Sci.*, vol. 26, no. 4, pp. 1119–1126, Aug. 1998.
- [14] S. Lee, S. H. Saw, P. Lee, and R. S. Rawat, "Numerical experiments on plasma focus neon soft X-ray scaling," *Plasma Phys. Control. Fusion*, vol. 51, no. 10, pp. 105013-1–105013-8, Oct. 2009.
- [15] M. Zakauallah, K. Alamgir, M. Shafiq, S. M. Hassan, M. Sharif, S. Hussain, and A. Waheed, "Characteristics of X-rays from a plasma focus operated with neon gas," *Plasma Sources Sci. Technol.*, vol. 11, no. 4, pp. 377–382, Nov. 2002.
- [16] H. Bhuyan, S. R. Mohanty, N. K. Neog, S. Bujarbarua, and R. K. Rout, "Comparative study of soft X-ray emission characteristics in a low energy dense plasma focus device," *J. Appl. Phys.*, vol. 95, no. 6, pp. 2975–2981, Mar. 2004.
- [17] F. N. Beg, I. Ross, A. Lorenz, J. F. Worley, A. E. Dangor, and M. G. Haines, "Study of X-ray emission from a table top plasma focus and its application as an X-ray backlighter," *J. Appl. Phys.*, vol. 88, no. 6, pp. 3225–3230, Sep. 2000.
- [18] M. Zakauallah, K. Alamgir, M. Shafiq, M. Sharif, and A. Waheed, "Scope of plasma focus with argon as a soft X-ray source," *IEEE Trans. Plasma Sci.*, vol. 30, no. 6, pp. 2089–2094, Dec. 2002.
- [19] M. Zakauallah, K. Alamgir, G. Murtaza, and A. Waheed, "Efficiency of plasma focus for argon K-series line radiation emission," *Plasma Sources Sci. Technol.*, vol. 9, no. 4, pp. 592–596, Nov. 2000.
- [20] D. Wong, A. Patran, T. L. Tan, R. S. Rawat, and P. Lee, "Soft X-ray optimization studies on a dense plasma focus device operated in neon and argon in repetitive mode," *IEEE Trans. Plasma Sci.*, vol. 32, no. 6, pp. 2227–2235, Dec. 2004.
- [21] V. A. Gribkov, A. Srivastava, P. L. C. Keat, V. Kudryashov, and S. Lee, "Operation of NX2 dense plasma focus device with argon filling as a possible radiation source for micro-machining," *IEEE Trans. Plasma Sci.*, vol. 30, no. 3, pp. 1331–1338, Jun. 2002.
- [22] M. Shafiq, Sartaj, S. Hussain, M. Sharif, S. Ahmad, M. Zakauallah, and A. Waheed, "Soft X-Ray emission in the (1.0–1.5 keV) window with nitrogen filling in a low energy plasma focus," *Mod. Phys. Lett. B*, vol. 16, no. 9, pp. 309–318, 2002.
- [23] M. Shafiq, S. Hussain, M. Sharif, and M. Zakauallah, "Soft X-ray emission optimization study with nitrogen gas in a 1.2 kJ plasma focus," *J. Fusion Energy*, vol. 20, no. 3, pp. 113–115, Sep. 2001.
- [24] N. K. Neog, S. R. Mohanty, and E. Hotta, "Anode length optimization in a modified plasma focus device for optimal X-ray yields," *J. Appl. Phys.*, vol. 99, no. 1, pp. 013302-1–013302-7, Jan. 2006.
- [25] A. Roomi, E. Saion, M. Habibi, R. Amrollahi, R. Baghdadi, G. R. Etaati, W. Mahmood, and M. Iqbal, "The effect of applied voltage and operating pressure on emitted X-ray from nitrogen (N₂) gas in APF plasma focus device," *J. Fusion Energy*, vol. 30, no. 5, pp. 413–420, Oct. 2011.
- [26] M. A. I. Elgarhy, "Plasma focus and its applications," M.Sc. thesis, Al-Azhar University, Cairo, Egypt, 2010.
- [27] R. Lebert, D. Rothweiler, A. Engel, K. Bergmann, and W. Neff, "Pinch plasmas as intense EUV source for laboratory applications," *Opt. Quantum Electron.*, vol. 28, no. 3, pp. 241–259, Mar. 1996.
- [28] F. Richter, J. Eberle, R. Holz, W. Neff, and R. Lebert, "Repetitive plasma focus as radiation source for X-ray lithography," in *Proc. 2nd Int. Conf. Dense Z-Pinches*, 1989, vol. 195, pp. 515–521.
- [29] R. Lebert, A. Engel, and W. Neff, "Investigations on the transition between column and micropinch mode of plasma focus operation," *J. Appl. Phys.*, vol. 78, no. 11, pp. 6414–6420, Dec. 1995.
- [30] L. Rico, B. J. Gomez, J. N. Feugeas, and O. de Sanctis, "Crystallization of amorphous zirconium thin film using ion implantation by a plasma focus of 1 kJ," *Appl. Surf. Sci.*, vol. 254, no. 1, pp. 193–196, Oct. 2007.
- [31] L. Rico, B. J. Gomez, M. Stachoitti, N. Pellegri, J. N. Feugeas, and 519 O. de Sanctis, "Oxygen ion implantation in strontium bismuth tantalate 520 thin films," *Braz. J. Phys.*, vol. 36, no. 3B, pp. 1009–1012, Sep. 2006. 521
- [32] Institute for Plasma Focus Studies. [Online]. Available: <http://www.plasmafocus.net> 522
- [33] "Internet Workshop on Plasma Focus Numerical Experiments (IPFS- 524 IBC1)," Apr. 14/May 19, 2008. [Online]. Available: www.plasmafocus.net/IPFS/Papers/IWPCAkeynote2ResultsOfInternet-basedWorkshop.doc 525
- [34] S. Lee, Radiative Dense Plasma Focus Computation Package: 527 RADPF, 2011. [Online]. Available: <http://www.plasmafocus.net/IPFS/528 modelpackage/FileIRADPF.htm>; <http://www.intimal.edu.my/school/fas/UFLF/> 529
- [35] S. Lee, R. S. Rawat, P. Lee, and S. H. Saw, "Soft X-ray yield from NX2 plas- 531 ma focus," *J. Appl. Phys.*, vol. 106, no. 2, pp. 023309-1–023309-6, Jul. 2009. 532
- [36] S. H. Saw and S. Lee, "Scaling laws for plasma focus machines from 533 numerical experiments," *Energy Power Eng.*, vol. 2, no. 1, pp. 65–72, 2010. 534
- [37] S. Lee, S. H. Saw, P. C. K. Lee, R. S. Rawat, and H. Schmidt, "Computing 535 plasma focus pinch current from total current measurement," *Appl. Phys. Lett.*, vol. 92, no. 11, pp. 111501-1–111501-3, Mar. 2008. 537
- [38] S. Lee and S. H. Saw, "Pinch current limitation effect in plasma focus," 538 *Appl. Phys. Lett.*, vol. 92, no. 2, pp. 021503-1–021503-3, Jan. 2008. 539
- [39] S. Lee, P. Lee, S. H. Saw, and R. S. Rawat, "Numerical experiments on 540 plasma focus pinch current limitation," *Plasma Phys. Control. Fusion*, vol. 50, no. 6, pp. 065012-1–065012-8, Jun. 2008. 542
- [40] K. N. Koshelev, V. I. Krauz, N. G. Reshetniak, R. G. Salukvadze, 543 Y. V. Sidelnikov, and E. Y. Khautev, "X-ray diagnostics of plasma focus 544 DPF-78 discharge," *J. Phys. D, Appl. Phys.*, vol. 21, p. 1827, 1988. 545
- [41] S. Lee, S. H. Saw, and J. Ali, "Numerical experiments on radiative cooling 546 and collapse in plasma focus operated in krypton," *J. Fusion Energy*, vol. 31, no. 1, pp. 1–8, Feb. 26, 2012. DOI:10.1007/s10894-012-9522-8. 547
- [42] S. Lee and S. H. Saw, "Multi-radiation modelling of the plasma fo- 549 cus," in *Proc. 5th Int. Conf. Frontiers Plasma Phys. Technol.*, Singapore, 550 Apr. 18–22, 2011. 551
- [43] Z. Ali, S. Lee, F. D. Ismail, Saktioto, J. Ali, and P. P. Yupapin, "Radiation 552 self absorption effect in Ar gas NX2 mather type plasma focus," *Proc. Eng.*, vol. 8, pp. 393–400, 2011. 554
- [44] S. Lee, "Radius ratios of argon pinches," *Aust. J. Phys.*, vol. 36, no. 6, 555 pp. 891–895, 1983. 556
- [45] M. H. Liu, "Soft X-Ray from compact plasma focus," Ph.D. dissertation, 557 Nanyang Technol. Univ., Singapore, Dec., 1996. 558
- [46] M. Akel, S. Al-Hawat, and S. Lee, "Numerical experiments on soft 559 X-ray emission optimization of nitrogen plasma in 3 kJ plasma focus SY-1 560 using modified Lee Model," *J. Fusion Energy*, vol. 28, no. 4, pp. 355–363, 561 Dec. 2009. 562
- [47] M. Akel, S. Al-Hawat, S. H. Saw, and S. Lee, "Numerical experiments 563 on oxygen soft X-ray emissions from low energy plasma focus using Lee 564 Model," *J. Fusion Energy*, vol. 29, no. 3, pp. 223–231, Jun. 2010. 565
- [48] M. Akel, S. Al-Hawat, and S. Lee, "Pinch current and soft X-ray yield 566 limitations by numerical experiments on nitrogen plasma focus," *J. Fusion Energy*, vol. 29, no. 1, pp. 94–99, Feb. 2010. 568
- [49] M. Akel, S. Al-Hawat, and S. Lee, "Neon soft X-ray yield optimization 569 from PF-SY1 plasma focus device," *J. Fusion Energy*, vol. 30, no. 1, 570 pp. 39–47, Feb. 2011. 571
- [50] M. H. Liu, X. Feng, S. V. Springham, and S. Lee, "Soft X-ray measure- 572 ment in a small plasma focus operated in neon," *IEEE Trans. Plasma Sci.*, vol. 26, no. 2, pp. 135–140, Apr. 1998. 574
- [51] S. H. Saw, P. C. K. Lee, R. S. Rawat, and S. Lee, "Optimizing UNU/ICTP 575 PFF plasma focus for neon soft X-ray operation," *IEEE Trans. Plasma Sci.*, vol. 37, no. 7, pp. 1276–1282, Jul. 2009. 577
- [52] M. Akel and S. Lee, "Practical optimization of AECS PF-2 plasma focus 578 device for argon soft x-ray operation," *J. Fusion Energy*, vol. 31, no. 2, 579 pp. 122–129, Apr. 2012. 580
- [53] M. Akel and S. Lee, "Dependence of plasma focus argon soft X-ray yield 581 on storage energy, total and pinch currents," *J. Fusion Energy*, vol. 31, 582 no. 2, pp. 143–150, Apr. 2012. 583
- [54] S. Al-Hawat, M. Akel, and C. S. Wong, "X-ray emission from argon 584 plasma focus contaminated with copper impurities in AECS PF-2 us- 585 ing five channel diode spectrometer," *J. Fusion Energy*, vol. 30, no. 6, 586 pp. 503–508, Dec. 2011. 587
- [55] S. Al-Hawat, M. Akel, S. H. Saw, and S. Lee, "Model parameters vs. 588 gas pressure in two different plasma focus devices operated in Argon and 589 Neon," *J. Fusion Energy*, vol. 31, no. 1, pp. 13–20, Feb. 2012. 590
- [56] S. Al-Hawat, "Axial velocity measurement of current sheath in a plasma 591 focus device using a magnetic probe," *IEEE Trans. Plasma Sci.*, vol. 32, 592 no. 2, pp. 764–769, Apr. 2004. 593
- [57] S. Al-Hawat, M. Soukieh, M. Abou Kharoub, and W. Al-Sadat, "Using 594 Mather-type plasma focus device for surface modification of AISI304 595 steel," *Vacuum*, vol. 84, no. 7, pp. 907–912, Mar. 2010. 596

- 597 [58] M. Habibi, R. Amrollahi, and M. Attaran, "Experimental study of cur-
598 rent discharge behavior and hard X-ray anisotropy by APF plasma focus
599 device," *J. Fusion Energy*, vol. 28, no. 1, pp. 130–134, 2009.
- 600 [59] R. A. Behbahani, T. D. Mahabadi, M. Ghoranneviss, M. F. Aghamir, S. E.
601 Namini, A. Ghorbani, and M. Najafi, "Study of plasma sheath dynamics
602 by using two magnetic probes in a low energy plasma focus device,"
603 *Plasma Phys. Control. Fusion*, vol. 52, no. 9, p. 095004, Sep. 2010.
- 604 [60] M. Zakaullah, K. Alamgir, M. Shafiq, M. Sharif, A. Waheed, and
605 G. Murtaza, "Low-energy plasma focus as a tailored X-ray source,"
606 *J. Fusion Energy*, vol. 19, no. 2, pp. 143–157, Jun. 2000.
- 607 [61] N. D. Farahani, F. A. Davani, and Z. S. Rad, "X-Ray measurement and
608 enhancement of SBUPF1 plasma focus device in different Ar pressures
609 and operating voltages," *J. Fusion Energy*, vol. 30, no. 6, pp. 466–472,
610 Dec. 2011.
- 611 [62] Z. Shahbazi rad, M. Shahriari, and F. Abbasi Davani, "Investigation of
612 spatial distribution of hydrogen and argon ions and effects of them on
613 aluminum samples in a 2.5 kJ mater type plasma focus device," *J. Fusion
614 Energy*, vol. 30, no. 5, pp. 358–366, Oct. 2011.
- 615 [63] S. Al-Hawat, M. Akel, and S. Lee, "Numerical experiments on Neon soft
616 X-ray optimization of AECS-PF2 plasma focus device," *J. Fusion Energy*,
617 vol. 30, no. 6, pp. 494–502, Dec. 2011.
- 618 [64] M. Akel, "Yield optimization of Helium and Lyman emissions in low
619 energy plasma focus operated with Argon," *J. Fusion Energy*, vol. 31,
620 no. 5, pp. 473–479, Oct. 2012.
- 621 [65] S. Lee, "Current and neutron scaling for megajoule plasma focus ma-
622 chines," *Plasma Phys. Control. Fusion*, vol. 50, no. 10, pp. 105005–1–
623 105005-14, Oct. 2008.
- 624 [66] S. Lee, "Neutron yield saturation in plasma focus—A fundamental cause,"
625 *Appl. Phys. Lett.*, vol. 95, no. 15, pp. 151503-1–151503-3, Oct. 2009.
- 626 [67] M. Akel and S. Lee, "Scaling laws of nitrogen soft X-ray yields from
627 1–200 kJ plasma focus," *J. Fusion Energy*, pp. 1–4, Mar. 30, 2012.
628 DOI:10.1007/s10894-012-9537-1.
- 629 [68] M. Akel and S. Lee, "Radiative collapse in plasma focus operated
630 with heavy noble gases," *J. Fusion Energy*, pp. 1–6, Mar. 31, 2012.
631 DOI:10.1007/s10894-012-9535-3.

632
633
634
635
636
637
638
639



Mohamad Akel received the M.Sc. and the Ph.D. degrees in plasma physics from the Moscow Engineering Physics Institute (State University), Moscow, Russia, in 2000 and 2004, respectively.

He is an Associate Professor at the Department of Physics, Plasma Division, Atomic Energy Commission of Syria. Currently, he is working in the plasma focus laboratory.



Sing Lee received the B.Sc. and M.Sc. degrees from the University of Malaya (UM), Kuala Lumpur, Malaysia, in 1964 and 1966, respectively and the Ph.D. degree from the Australian National University, Canberra, Australia, in 1970.

He was a Professor of Applied Physics and headed research groups in Plasma and Pulse Technology and the Physics Department at UM and was Head of Division of Physics and Head Academic Group of Natural Sciences at Nanyang Technological University, National Institute of Education, Singapore. He was Alexander von Humboldt Fellow (1975–1976) at Kernforschungslange, Juelich, West Germany, Commonwealth Academic Staff Fellow (1981–1982) at Imperial College, London, and Visiting Professor and United Nations University Special Fellow (1986–1987) at Flinders University of South Australia. He was the Founder President of the Asian African Association for Plasma Training (AAAPT), the Associate Director of the AAAPT Research and Training Centre of the Institute of Physics, Academia Sinica, Beijing, Far Eastern Representative of the International Centre for Theoretical Physics, and ardent advocate and implementor of south–south technology creation and transfer, especially in plasma fusion, laser, and pulse technology. A Chartered Physicist and Fellow of the Institute of Physics (U.K.), Life and Hon Fellow of the Institute of Physics Malaysia, and Life Fellow of the Singapore Institute of Physics and the Samahang Pisika ng Pilipinas, he is the Founder Principal of the (web-based) Institute for Plasma Focus Studies, Melbourne, Adjunct Professor (honorary) INTI International University, Malaysia and Emeritus Professor, University of Malaya.



S. H. Saw received the B.Sc.(Hons) and Ph.D. degrees in physics from the University of Malaya (UM) in 1985 and 1991, respectively, and M.A. degree in educational management from the University of Nottingham, U.K., in 1997.

She is a Professor and the Pro Vice Chancellor of INTI International University, Nilai, Malaysia, and also the Director of its Centre for Plasma Research. She is Co-Director of the Institute of Plasma Focus Studies, Melbourne, Australia, and the designated delegate of INTI IU for Asian African Association for Plasma Training. Her current research interests include plasma physics and teaching quality and innovation.